Quantum Mechanical Cluster Calculations of Critical Scintillation Processes*

Stephen E. Derenzo, Mattias K. Klintenberg, and Marvin J. Weber

Lawrence Berkeley National Laboratory, Berkeley, CA 94720, U. S. A.

This paper describes the use of commercial quantum chemistry codes to simulate several critical scintillation processes. The crystal is modeled as a cluster of typically 50 atoms embedded in an array of typically 5,000 point charges designed to reproduce the electrostatic field of the infinite crystal. The Schrödinger equation is solved for the ground, ionized, and excited states of the system to determine the energy and electron wavefunction. Computational methods for the following critical processes are described: (1) the formation and diffusion of relaxed holes, (2) the formation of excitons, (3) the trapping of electrons and holes by activator atoms, (4) the excitation of activator atoms, and (5) thermal quenching. Examples include hole diffusion in CsI, the exciton in CsI, the excited state of CsI:Tl, the energy barrier for the diffusion of relaxed holes in CaF_2 and PbF_2, and prompt hole trapping by activator atoms in CaF_2:Eu and CdS:Te leading to an ultra-fast (< 50 ps) scintillation risetime.

Keywords: Quantum mechanical calculations, Embedded cluster method, Hole diffusion, Prompt excitation, Thermal quenching, CsI, CsI:Tl, CaF_2:Eu, CdS:Te, PbF_2,

1. Introduction

This work is motivated by the need for a bright, fast, dense, heavy-atom scintillator for time-of-flight positron emission tomography in molecular nuclear medical imaging. It focuses on processes that quickly and efficiently convert ionization energy into useful optical photons. Since there are over 4,000 candidate host materials with good photoelectric stopping power and a suitable band gap, and each can be doped with many activators in different concentrations, a purely experimental search would involve synthesizing and testing an enormous number of samples! This is not practical, but fortunately the computational guidance that we need is now becoming accessible through modern quantum chemistry computer codes and faster computers.

The *theory* for these calculations is on solid mathematical footing, as almost all of solid state physics can be described by the Schrödinger equation, but numerical solutions of this equation for systems of realistic size are a serious challenge. Clearly, if computer speed continues to expand as it has in the recent past, it will be possible to model at the molecular level more and more of the processes important to a wide variety of technologies. This work is an attempt to see how well we can model known scintillators at the current time.

Section 2 describes processes critical for fast, efficient scintillation, computational procedures for modeling them, and the computer resources required. Section 3 shows some examples of how these methods can be applied to known scintillators and Section 4 discusses the

* U.S. DOE Contract DE-AC03-76SF00098 & U.S. NIH grant R01-CA48002

possibilities for improvements in hardware and software and the use of quantum simulations to guide the search for new scintillators.

2. Scintillation Processes and Computational Methods

2.1 Scintillation Processes

Scintillation can be described in three stages [1, 2], with an overall luminous efficiency η (photons per MeV) given by

$$\eta = \gamma S q \tag{1}$$

where γ is the number of electrons and holes produced per MeV of ionizing radiation, S is the efficiency with which the electrons and holes transfer their energy to the luminescent center, and q is the quantum efficiency of the excited state of the luminescent center.

The first stage is the production of separated electrons and holes by an energetic charged particle. This occurs in all crystals and the energy needed to create an electron-hole pair is typically three times the band gap of the crystal.

The second stage is the formation of an excited state. Here we distinguish four major types of scintillators: (1) the intrinsic scintillator, where the excitation occurs when an electron moves in the conduction band and becomes bound to a relaxed hole to create an exciton, (2) the self activated scintillator, where the electron and hole are both trapped on a luminous atom that is a major constituent of the crystal, (3) the scintillator with an electron-trapping activator atom that first traps an electron and then traps a relaxed hole to become excited, and (4) the scintillator with a hole-trapping activator atom that first traps a hole and then traps an electron to become excited.

The third stage is the return of the excited state to the ground state, either through the emission of a photon or through the production of phonons (heat). For a more complete treatment of these and many other scintillation mechanisms, see reference [2].

Of the many undoped and doped host crystals that have ever been tested, very few produce useful scintillation. The critical processes that distinguish these few include (1) the efficient excitation of activator atoms by the sequential trapping of electrons and holes, (2) for electron-trapping activators, the ability of relaxed holes to efficiently diffuse through the host crystal to an activator atom that has trapped an electron, and (3) minimal thermal quenching of the excited states.

2.2 The Embedded Quantum Mechanical Cluster Method

The embedded quantum mechanical cluster method is one of the most powerful methods for modeling solid state systems [3]. Among other features, it permits calculations of systems that have nonzero charge. It is compatible with commercial quantum chemistry programs even though they were generally designed for molecules rather than crystals.

In this method the crystal is modeled as a central cluster of typically 20 to 60 atoms embedded in a lattice of point charges designed to reproduce the electrostatic field of the infinite crystal. To explore scintillation processes, the Schrödinger equation is solved (at some level of approximation) to determine the energy and electronic configuration of the cluster (1) in

the ground state, (2) with a missing electron, (3) with an extra electron, and (4) in an electronic excited state.

A large array of unit cells does not accurately reproduce the electrostatic potential of the infinite crystal field. As the number of unit cells in the array is increased, the potentials in the central volume of the array asymptotically reach limiting values that can disagree with the values given by the Ewald summation formula [4] by many eV. Even the Evjen method [5], which can eliminate the dipole moment for many crystals by using fractional charges at the edges of the unit cell, generates potentials with a large additive potential error. We have developed a method for optimizing point charge arrays for any crystal whose crystal structure is known [6]. It is more accurate and more automatic than previous methods [7, 8] and has errors less than 1 μV within the volume of a typical 50-atom cluster.

Crystal structure data can be obtained, for example, from the Inorganic Crystal Structure Database (Karlsruhe). This is one of most complete reference of its kind and is readily found on the internet by searching for ICSD.

2.3 The Schrödinger Equation

A quantum mechanical system is described by its wavefunction Ψ, which is a complex function (real and imaginary parts) of the three Cartesian coordinates of all of its particles. $\Psi^*\Psi$ is the joint probability of all the particles in the system being at particular points in space. For N particles, the wavefunction is a function of $3N$ spatial coordinates, and for a stable (time invariant) system must obey the Schrödinger equation $H\,\Psi = E\,\Psi$, where H is a Hamiltonian operator that is the sum of a kinetic operator $\sum(1/m_i)(\partial^2/dx_i^2 + \partial^2/dy_i^2 + \partial^2/dz_i^2)$ and a potential term $\sum\sum q_i q_j / r_{ij}$ and E is the energy of the system. This equation has many solutions, and the ground state is the solution with the lowest energy.

In the Hartree-Fock method, each electron i is described by a molecular orbital ψ_i (a function of three spatial coordinates), and Ψ is the product of all orbitals summed over all antisymmetric permutations of electron assignment. This complication is necessary because the wavefunction must change sign if any two electrons are interchanged. Each molecular orbital ψ_i is approximated as a linear combination of basis functions, and each basis function ϕ_k is expanded by a linear combination of products of primitive Gaussian functions and polynomials that describe the s, p_x, p_y, p_z, etc. nature of the orbital.

$$\psi_i = \sum_{k=1}^{N} c_{ki}\,\phi_k \qquad (2)$$

The molecular orbital theory was a major step in the numerical solution of the Schrödinger equation (for which Mulliken won the Nobel prize in 1966). The Hartree-Fock method solves the Schrödinger equation by numerically optimizing one molecular orbital at a time, assuming at each step that the others are frozen. It ignores the dynamic electron correlation effects, which increase the strength of covalent bonds. On the other hand, it satisfies antisymmetric exchange perfectly, which decreases the strength of covalent bonds. As a result, the pure Hartree-Fock solution emphasizes ionic bonds and does not properly simulate the covalent bonds between two halogen atoms that share a hole to form a V_k center. Møller-Plesset second order correlation corrections (MP2) more properly show the bonding between the two halogen atoms in a V_k center. This was pointed out for the case of the NaCl

crystal in reference [9]. Higher orders of correction (MP3 and MP4) are available, but the computational cost is so high that they are only useful for small (few atom) systems.

Another computational approach for including the correlation energy is the configuration interaction method, which describes the wavefunction as a linear combination of occupied and unoccupied Hartree-Fock solution orbitals. The lowest level of this method that includes a correlation correction is called configuration interaction doubles (CID), where all possible double substitutions of occupied with unoccupied orbitals are used. The inclusion of single substitutions produces CISD and the inclusion of triple substitutions produces CISDT. While this approach is effective for small (few atom) systems, the computational cost is so high for large systems that it has largely been replaced by Density Functional Theory (DFT).

DFT introduces approximate exchange and correlation functionals to the Hamiltonian and provides some correlation correction at the computational cost of a simple Hartree-Fock calculation. DFT is much more economical than Møller-Plesset and configuration interaction methods and has provided correlation corrections to much larger systems than were previously possible. (For the development of DFT, Kohn and Pople won the Nobel Prize in 1998.)

For heavy atoms, the inner electrons are relativistic and cannot be accurately modeled by the Schrödinger equation. However they do not play a direct role in chemical reactions and electronic excitations but rather an indirect role in defining a core potential that the outer electrons experience. In actual practice, the non-relativistic Schroedinger equation is solved for only the outermost electrons, and the inner electrons that are most strongly affected by relativity are handled by effective core potentials (ECPs) that were determined by solving the Dirac equation for the isolated atom. Quantum chemistry programs provide libraries of basis functions (called basis sets) and some of these include ECPs for atoms heavier than Ne. For atoms heavier than Ar only basis sets with ECPs are available and only the outermost valence electrons are treated quantum mechanically (typically 4 to 14 per atom).

For excited states and for excess electrons in the conduction band, diffuse basis functions must be added to the standard basis sets to describe the diffuse nature of the electrons involved. The addition of diffuse basis functions lowers the energy of the excited state relative to the ground state and results in more accurate molecular orbitals and excitation energies. See references [10] and [11] for more information on modern quantum chemistry.

2.4 The Configuration Space of Atomic Positions

When the cluster has an impurity atom, a non-zero charge, or is in an excited state the normal lattice positions of the atoms is not the configuration of lowest energy. To find the lowest energy, the forces dE/dx_i, dE/dy_i, dE/dz_i are computed for each moveable atom *i* and the atoms are moved to minimize those forces. One useful and realistic assumption is the Born-Oppenheimer approximation, which states that the electrons are much lighter and move much faster than the nuclei and as a result they move with the nuclei. A more mathematical description is that the Schrödinger equation does not need to include the velocities of the nuclei because they are moving relatively slowly, and a valid energy minimum can be found by computing the energies and forces at stationary points in the configuration space.

Figure 1 shows the energy of a system in the ground and excited states as a function of a generalized configuration coordinate. The system starts in the relaxed ground state, is excited, and then relaxes geometrically in an electronic excited state. After a photon is emitted, the system is in a distorted configuration of the ground state and quickly relaxes. This makes it plausible that the absorption edge energy (up arrow) is more energetic than the emission (down arrow) energy.

Figure 1 also helps to explain thermal quenching, which occurs when the excited state configuration can be distorted by thermal vibrations to a possible ground state configuration. Here it is important to understand that the single horizontal axis coordinate shown is in reality a very large space of the spatial coordinates of all the atoms in the system. The overlap between the excited and ground states is not just the point where the curves cross in the figure, but a large subspace. One elegant way of solving for the quenching temperature is to use the Hessian matrix of second derivatives of the energy (a_{ij}) that is generated during the geometrical optimization. It can be used to parameterize the energy as a function of atom coordinates:

$$E = E_0 + \sum_{i=1}^{3N}\sum_{j=1}^{3N} a_{ij}(u_i - \bar{u}_i)(u_j - \bar{u}_j) \qquad (3)$$

where the variable u_i stands for the x, y, and z Cartesian coordinates of the atoms. Usually this matrix is diagonalized to find the vibrational modes and frequencies but it also provides analytical expressions for the energy surface of the ground and excited states. In these terms the thermal energy required for quenching can be estimated as the difference between (1) the minimum energy in the configuration space where the ground and excited state energies are equal (level crossing) and (2) the minimum energy of the excited state.

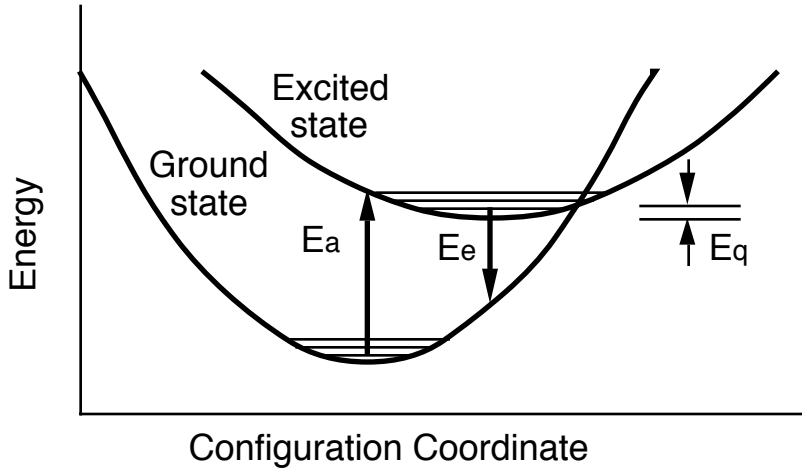

Figure 1. Configuration coordinate diagram (energy vs. atom positions) showing the absorption of a photon of energy E_a from the ground state, the emission of a photon of energy E_e from the relaxed excited state to a distorted ground state, and the thermal quenching energy E_q needed to distort the geometry of the excited state to a possible distorted ground state geometry.

2.5 Computational Requirements

Let us consider a system of N_a atoms with N_e quantum electrons per atom and an average of N_b basis functions centered on each of the N_a atoms. There are then N_a x N_e molecular orbitals and each is expanded as a linear combination of N_b x N_a basis functions. This means that the Schrödinger equation determines the wavefunction Ψ by N_a^2 N_b N_e expansion coefficients, and that the Hamiltonian matrix consists of N_a^4 N_b^2 N_e^2 elements, which is one measure of the computational effort. Since the number of atoms N_a scales as the cube of the diameter *D* of the atomic cluster, the computational effort scales as the twelfth power of *D*! In practice, the scaling exponent is reduced somewhat by the use of molecular symmetry and the selective updating of matrix elements between iterations.

Considering a typical system described in this paper, we have $N_a = 50$, $N_e = 10$, and $N_b = 10$. The wavefunction is described by 250,000 expansion coefficients and the Hamiltonian matrix contains $250{,}000^2$ or over 6×10^{10} elements. Solving the Hartree-Fock equation takes approximately 50 hours on a Silicon Graphics, Inc. R10k processor which during this time is operating at typically 250×10^6 floating point operations/s for a total of 10^{15} floating point operations. Dividing these two numbers gives an indication that approximately 20,000 floating point operations are required per matrix element to solve the equation.

Geometrical optimizations require typically 10 to 20 iterations of atom coordinate changes, and each iteration requires the solution of the Hartree-Fock equation and the determination of the new Hessian matrix. Fortunately, as the process converges, the changes in the atom positions decrease, and the time required for each Hartree-Fock solution also decreases. As a general rule, a geometrical optimization takes about ten times longer than the initial energy solution of the Hartree-Fock equation.

For the examples described below, we have used both the Gaussian94 (a product of Gaussian, Inc., Pittsburgh, PA, U.S.A.) and the Jaguar (a product of Schrodinger, Inc., Portland, OR, U.S.A.) quantum chemistry codes on a local cluster of twelve R10k processors (Silicon Graphics, Inc.) and on the U.S. Department of Energy National Energy Research Supercomputer Center J-90 processors (Silicon Graphics, Inc.).

3. Examples

3.1 Hole Relaxation and Diffusion in CsI

A relatively small CsI cluster with a missing electron readily exhibits the V_k center, which is a hole shared by two covalently bonded I ions [12, 13, 14]. By making the cluster large enough to describe a V_k center at two equivalent nearest neighbor sites, the minimum energy path in atomic configuration space can be determined. In CsI the transition configuration between two V_k centers is a single-center hole. The energy difference between these two states is the barrier for relaxed hole diffusion in the 0° direction. Using a $Cs_{16}I_{29}$ cluster and MP2 correlation corrections, the barrier energy was predicted to be 0.15 eV [13]. A larger $Cs_{32}I_{33}$ cluster that allows a more complete relaxation gives a barrier of 0.23 eV, in excellent agreement with an experimental value of 0.23 eV, determined by measuring the risetime of CsI:Tl which varied from 890 ns to 13 ns from –60 to +50 °C [15].

3.2 Excitons in CsI

Plots of the two unpaired electron orbitals in excited (triplet) CsI show that the lower half-filled orbital has the same spatial distribution as the V_k center, and that the upper half-filled orbital is spatially diffuse. The excited state is the expected exciton, an e^--V_k center [16].

3.3 The excited state in CsI:Tl

The excited state of CsI:Tl was found to be localized entirely on the Tl atom both in a $TlCs_{19}I_{20}$ and a larger $TlCs_{31}I_{33}$ cluster. The slow risetime indicates that the Tl^+ ion first traps an electron and the relaxed hole diffuses to it to form the excited Tl^+ state [16].

3.4 Energy Barriers for Relaxed Hole Diffusion in CaF_2 and PbF_2

Calculations of relaxed hole transport in the $Ca_{16}F_{32}$ and $Pb_{16}F_{32}$ clusters using Hartree Fock and MP2 predict energy barriers of 0.21 eV and 1.1 eV [17], respectively. The barrier height for CaF_2 is in fair agreement with the experimental value of 0.31 eV [18].

3.5 Prompt Hole Trapping and Ultra-Fast Risetimes in CaF_2:Eu and CdS:Te

Using our 100-ps pulsed x-ray system [19, 20] we have deconvolved the impulse response and measured of the risetime of the luminous (24,000 photons/MeV) scintillator CaF_2:Eu to be less than 50 ps. This is incompatible with the diffusion time of relaxed holes in CaF_2, which we estimate to be longer than 1 μs at room temperature using the data of reference [18]. We are forced to conclude that the Eu^{2+} activator ions promptly trap almost all the available holes before they can relax and that the free electrons are then quickly trapped to rapidly and efficiently form the Eu^{2+} excited state.

To model this behavior, quantum calculations were performed on the ground and hole states of the clusters $Ca_{16}F_{32}$ and $EuCa_{15}F_{32}$ using three different sets of DFT exchange and correlation functionals. The ionization potential of Ca_5F_{10} ranged from 10.0 to 11.0 eV (average 10.4 eV) and the ionization potential of $EuCa_4F_{10}$ ranged from 8.2 to 10.0 eV (average 9.2 eV). From these energy values and the diagram in Figure 2 we see that the Eu atom has electrons whose energies are just above the top of the valence band and that it is plausible that holes transfer promptly to the Eu^{2+} activator ion. The electron affinity for Ca_5F_{10} ranged from 1.2 to 1.4 eV (average 1.3 eV) and the electron affinity for $EuCa_4F_{10}$ ranged from 1.2 to 1.5 eV (average 1.4 eV). Thus it is plausible that the activator atoms have no electron affinity until they have trapped a hole.

Because CdS:Te is a luminous scintillator under electron beam excitation at temperatures as low as 1.6 K [21], it is unlikely that the diffusion of relaxed holes plays a role in the excitation of the activator. Moreover, our pulsed x-ray system measures the risetime to be less than 50 ps at room temperature.

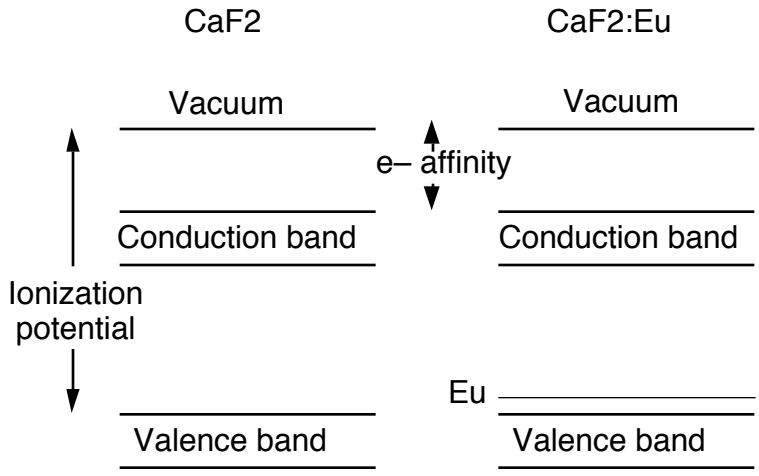

Figure 2 Band diagram for CaF_2 and CaF_2:Eu for the case where the ionization potential of CaF_2:Eu is slightly less than that of CaF_2.

To see if the quantum calculations support this interpretation, activator affinity calculations were performed on $Cd_{13}S_{13}$ and $Cd_{13}S_{12}Te$ clusters. The ionization potential for $Cd_{13}S_{13}$ ranged from 9.6 to 10.1 eV (average 9.8 eV) and the ionization potential for $Cd_{13}S_{12}Te$ ranged from 9.3 to 9.6 eV (average 9.5 eV). Here we see that Te has an electron whose energy is just above at the top of the valence band and that it is plausible that holes transfer promptly to the Te activator ion. The electron affinity for $Cd_{13}S_{13}$ ranged from 3.7 to 4.1 eV (average 3.9 eV) and the electron affinity for $Cd_{13}S_{12}Te$ ranged from 3.7 to 4.1 eV (average 3.9 eV). Thus in this case too it is plausible that the activator atoms have no electron affinity until they have trapped a hole.

4. Discussion

This work shows that it is possible to use the embedded quantum mechanical cluster method to model a number of important scintillation mechanisms. Combining these results with experimental data can yield an improved understanding of scintillation mechanisms and the ability to simulate scintillation in families of host crystals and activator atoms and thus guide the experimental search Figure 3).

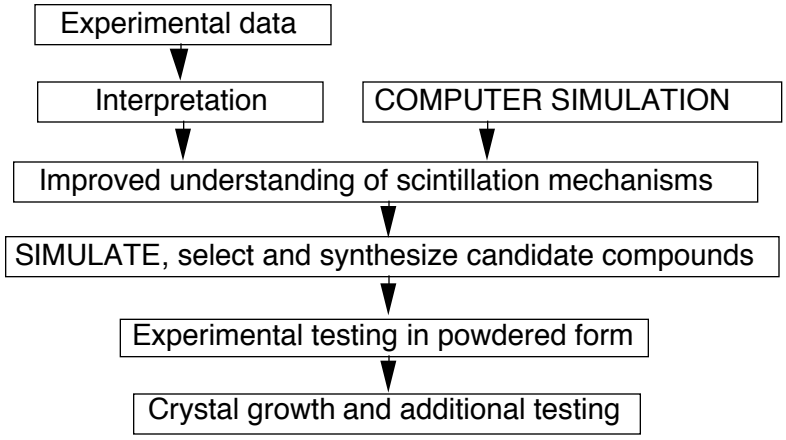

Figure 3. Role of quantum calculations in improving the understanding of scintillation mechanisms and in aiding the search for new scintillators.

The experimental data showing the ultra-fast risetime of CaF_2:Eu and CdS:Te and the computational prediction of prompt hole trapping by the corresponding activator atoms is a good example of the combined power of experiment and simulation.

The future of this work is limited by computational speed and the ability of the software to model crystal systems. While computer speed continues to increase at a spectacular rate, improvements in software are largely driven by applications in organic chemistry and for the catalysis of chemical reactions. More effort is needed to improve quantum chemistry codes to (1) increase the robustness of convergence for ionic systems and (2) support pseudo atoms that have the force properties of ground-state quantum atoms without having to include their electrons in the quantum calculation. Such improvements in software alone could speed the calculation by factors of 10 to 100 or improve the accuracy by allowing the use of more basis functions or a higher level of theory. The results described here represent only a small sampling of what will be possible in the future.

5. Acknowledgments

We thank W. Moses, K. Song, P. Gill, E. Heifets, R. Deich, J. Hay, and W. Goddard for helpful discussions and M. Ringnalda, G. Vacek, W. Pollard, J. Perry and R. Murphy for advice on the use of the Jaguar program. This work was supported in part by the Director, Office of Science, Office of Biological and Environmental Research, Medical Science Division of the U.S. Department of Energy under contract No. DE-AC03-76SF00098, in part by the U.S. Department of Energy National Energy Research Supercomputer Center, and in part by the National Institutes of Health, National Cancer Institute under grant No. R01-CA48002. Reference to a company or product name does not imply approval or recommendation by the University of California or the U.S. Department of Energy to the exclusion of others that may be suitable.

6. References

1. G. Blasse, Scintillator Materials, Chem Matter, **6** (1994), 1465-1475
2. P.A. Rodnyi. Physical Processes in Inorganic Scintillators. pp. 219, CRC Press (ISBN 0-8493-3788-7), Boca Raton, FL, 1997
3. R.W. Grimes, C.R.A. Catlow, and A.L. Shluger, Quantum mechanical cluster calculations in solid state studies, World Scientific, Singapore, 1992
4. P. Ewald, Die berechnung optischer und elektrostatischer gitterpotentiale, Ann Phys (Leiptzig), **64** (1921), 253-287
5. H.M. Evjen, Phys Rev, **39** (1932), 675
6. S.E. Derenzo, M.K. Klintenberg, and M.J. Weber, Determining point charge arrays that produce accurate ionic crystal fields for atomic cluster calculations, J Chem Phys (submitted), (1999),
7. C. Sousa, J. Casanovas, J. Rubio, and F. Illas, Madelung fields from optimized point charges for *ab initio* cluster model calculations on ionic systems, J Comp Chem, **14** (1993), 680-684
8. E.V. Stefanovich, and T.N. Thuong, A simple method for incorporating Madelung field effects into ab initio embedded cluster calculations of crystals and macromolecules, J Phys Chem B, **102** (1998), 3018-3022
9. V.E. Puchin, A.L. Shluger, and H. Itoh, Electron correlation in the self-trapped hole and exciton in the NaCl crystal, Phys Rev B, **52** (1995), 6254-6264

10. A. Szabo, and N.S. Ostlund. Modern Quantum Chemistry. pp. 466, Dover Publications, Inc., Mineola, NY, 1989
11. W.J. Hehre, L. Radom, P.v.R. Schleyer, and J.A. Pople. Ab Initio Molecular Orbital Theory. pp. 548, John Wiley & Sons, New York, 1986
12. S.E. Derenzo, and M.J. Weber, Ab-initio cluster calculations of hole transport and activator excitation in CsI:Tl and CsI:Na, IEEE Nuclear Science Symposium Conference Record (CD-ROM ISBN 0-7803-4261-5), (1997),
13. S.E. Derenzo, and M.J. Weber. Ab-initio calculations of hole transport and activator excitation in CsI:Tl and CsI:Na. Proceedings of The SCINT97: International Conference on Inorganic Scintillators and Their Applications, 103-106, (Edited by Y. Zhiwen, L. Peijun, F. Xiqi and X. Zhilin), Shanghi, P.R. China, 1997
14. S.E. Derenzo, and M.J. Weber, Prospects for first principle calculations of scintillator properties, Nucl Instr Meth A, **422** (1999), 111-118
15. J.D. Valentine, W.W. Moses, S.E. Derenzo, D.K. Wehe, and G.F. Knoll, Temperature dependence of CsI(Tl) gamma-ray scintillation decay time constants and emission spectrum, Nucl Instr Meth, **A325** (1993), 147-157
16. S.E. Derenzo, M. Klintenberg, and M.J. Weber. *Ab-initio* computations of hole transport and excitonic processes in inorganic scintillators. Proceedings of The Third International Conference on Excitonic Processes in Condensed Matter (EXCON '98), PV 98-25 (ISBN 1-56677-219-2), 391-402, (Edited by R. T. Williams and W. M. Yen), Boston, 1998
17. S.E. Derenzo, M. Klintenberg, and M.J. Weber, Ab-initio cluster calculations of hole trapping in PbF_2 and PbF_4, 1999 IEEE Trans Nucl Sci (submitted), **NS-46** (1998),
18. J.H. Beaumont, W. Hayes, D.L. Kirk, and G.P. Sommers, An investigation of trapped holes and trapped excitons in alkaline earth fluorides, Proc Roy Soc Lond, **A315** (1970), 69-97
19. S.E. Derenzo, W.W. Moses, S.C. Blankespoor, M. Ito, and K. Oba, Design of a pulsed x-ray system for fluorescent lifetime measurements with a timing resolution of 109 ps, IEEE Trans. Nucl. Sci., **NS-41** (1994), 629–631
20. S.C. Blankespoor, S.E. Derenzo, W.W. Moses, C.S. Rossington, M. Ito, and K. Oba, Characterization of a pulsed X-ray source for fluorescent lifetime measurements, IEEE Trans Nucl Sci, **NS-41** (1994), 698-702
21. J.D. Cuthbert, and D.G. Thomas, Optical properties of Tellurium as an isoelectonic trap in cadmium sulfide, J Appl Phys, **39** (1968), 1573-1580